



# Mutagenesis of odorant coreceptor *Orco* fully disrupts foraging but not oviposition behaviors in the hawkmoth *Manduca sexta*

Richard A. Fandino<sup>a,1,2,3</sup>, Alexander Haverkamp<sup>a,3,4</sup>, Sonja Bisch-Knaden<sup>a</sup>, Jin Zhang<sup>a</sup>, Sascha Bucks<sup>a</sup>, Tu Anh Thi Nguyen<sup>a,5</sup>, Katrin Schröder<sup>b</sup>, Achim Werckenthin<sup>b</sup>, Jürgen Rybak<sup>a</sup>, Monika Stengl<sup>b</sup>, Markus Knaden<sup>a,6</sup>, Bill S. Hansson<sup>a,2,6</sup>, and Ewald Große-Wilde<sup>a,6,7</sup>

<sup>a</sup>Department of Evolutionary Neuroethology, Max Planck Institute for Chemical Ecology, D-07745 Jena, Germany; and <sup>b</sup>Department of Animal Physiology, University of Kassel, D-34132 Kassel, Germany

Edited by John G. Hildebrand, University of Arizona, Tucson, AZ, and approved June 24, 2019 (received for review February 5, 2019)

The hawkmoth *Manduca sexta* and one of its preferred hosts in the North American Southwest, *Datura wrightii*, share a model insect–plant relationship based on mutualistic and antagonistic life-history traits. *D. wrightii* is the innately preferred nectar source and oviposition host for *M. sexta*. Hence, the hawkmoth is an important pollinator while the *M. sexta* larvae are specialized herbivores of the plant. Olfactory detection of plant volatiles plays a crucial role in the behavior of the hawkmoth. In vivo, the odorant receptor coreceptor (*Orco*) is an obligatory component for the function of odorant receptors (ORs), a major receptor family involved in insect olfaction. We used CRISPR-Cas9 targeted mutagenesis to knock out (KO) the *MsexOrco* gene to test the consequences of a loss of OR-mediated olfaction in an insect–plant relationship. Neurophysiological characterization revealed severely reduced antennal and antennal lobe responses to representative odorants emitted by *D. wrightii*. In a wind-tunnel setting with a flowering plant, *Orco* KO hawkmoths showed disrupted flight orientation and an ablated proboscis extension response to the natural stimulus. The *Orco* KO gravid female displayed reduced attraction toward a nonflowering plant. However, more than half of hawkmoths were able to use characteristic odor-directed flight orientation and oviposit on the host plant. Overall, OR-mediated olfaction is essential for foraging and pollination behaviors, but plant-seeking and oviposition behaviors are sustained through additional OR-independent sensory cues.

*Manduca sexta* | *Orco* | CRISPR-Cas9 | insect olfaction | insect–plant interactions

Chemical signals are important for feeding and reproductive behaviors in insects and are major drivers of insect–plant interactions (1, 2). In the North American Southwest, *Datura wrightii* has a relationship with the hawkmoth *Manduca sexta* based on pollination and herbivory (3–5). Large and light-reflective *D. wrightii* flowers advertise nectar through a fragrant volatile blend and are an innately preferred nectar source for foraging *M. sexta* (5, 6). Both visual and olfactory cues of the upright trumpet flower guide foraging decisions, indicated by hovering and an unfurling proboscis (7, 8). The hovering hawkmoth with extended proboscis is capable of close-range olfactory (9) and mechanosensory (10) guidance to reach the nectar canals. Field and laboratory observations found that females intersperse feeding bouts with oviposition (7, 11, 12) and *M. sexta* females have innate attraction not only to flowering but also to nonflowering *D. wrightii* plants (13). Plant volatiles elicit orientation and odor-directed flight in the female hawkmoth (13–15), followed by tarsal contact and abdomen-curling behavior, likely recognizing contact chemosensory cues eliciting oviposition (16). Plants are also capable of manipulating insect behavior through modulation of the volatile blend. For example, herbivore-induced volatiles may facilitate attraction of the natural enemies of the herbivore (17–19) or repel a gravid female (20–22). Therefore,

olfactory-directed behaviors are critical toward the survival of both insect and plant host.

The antennal response toward odorants determines a very well characterized moth behavior involving surge and casting upwind flight toward the odorant source (23). While largely described for pheromone-directed behaviors, the distribution of odorant plumes and perception of plant volatiles in flight would theoretically parallel mate-seeking behaviors (14, 24, 25). *D. wrightii* produces a large repertoire of plant volatile compounds and the *M. sexta*

## Significance

Insects detect plant volatiles mainly through the expression of odorant receptors (ORs) and ionotropic receptors (IRs) in olfactory sensory neurons. In vivo, *Orco* is an obligate partner for OR but not for IR function. We applied CRISPR-Cas9 in the hawkmoth *Manduca sexta* to mutate the *Orco* gene and investigate the physiological and behavioral implication of a loss of *Orco* receptor function in a semiecological interaction with its preferred host plant, the Western Jimsonweed, *Datura wrightii*. We found foraging behaviors were largely disrupted. Oviposition behaviors were also affected, but the hawkmoth was capable of exhibiting directed flight toward the nonflowering plant. These results enhance our understanding on the olfactory basis of insect–plant interactions shaping our ecological and agricultural landscapes.

Author contributions: R.A.F., A.H., M.K., B.S.H., and E.G.-W. designed research; R.A.F., A.H., S.B.-K., J.Z., S.B., T.A.T.N., K.S., A.W., and M.S. performed research; R.A.F., A.H., and S.B. contributed new reagents/analytic tools; R.A.F., A.H., S.B.-K., J.R., and M.K. analyzed data; and R.A.F., A.H., S.B.-K., M.S., B.S.H., and E.G.-W. wrote the paper.

The authors declare no conflict of interest.

This article is a PNAS Direct Submission.

This open access article is distributed under [Creative Commons Attribution-NonCommercial-NoDerivatives License 4.0 \(CC BY-NC-ND\)](https://creativecommons.org/licenses/by-nc-nd/4.0/).

Data deposition: All data and R-scripts are available at the Max Planck Repository: <https://edmond.mpdl.mpg.de/imeji/collection/MTBbtaiulvOibV4q>.

<sup>1</sup>Present address: Mass Spectrometry Group, Max Planck Institute for Chemical Ecology, D-07745 Jena, Germany.

<sup>2</sup>To whom correspondence may be addressed. Email: rfandino@ice.mpg.de or hansson@ice.mpg.de.

<sup>3</sup>R.A.F. and A.H. contributed equally to this work.

<sup>4</sup>Present address: Laboratory of Entomology, Wageningen University, 6708 PB Wageningen, The Netherlands.

<sup>5</sup>Present address: Lehrstuhl für Zoologie II, University of Würzburg, D-97074 Würzburg, Germany.

<sup>6</sup>M.K., B.S.H., and E.G.-W. contributed equally to this work.

<sup>7</sup>Present address: Faculty of Forestry and Wood Sciences, Czech University of Life Sciences, 165 00 Prague, Czech Republic.

This article contains supporting information online at [www.pnas.org/lookup/suppl/doi:10.1073/pnas.1902089116/-DCSupplemental](http://www.pnas.org/lookup/suppl/doi:10.1073/pnas.1902089116/-DCSupplemental).

Published online July 18, 2019.

antennae are tuned to many of these compounds (15, 26–29). The perception of floral volatile blends from *Datura* elicit a characteristic odor-directed flight behavior in *M. sexta*, shaping the odor-directed flight perception of floral plumes in an olfactory complex natural environment (29, 30). However, several plant-derived single compounds from *Datura* evoke upwind flight and foraging behavior in *M. sexta*, while oviposition behaviors seem to depend more on the detection of plant volatile mixtures (31). The hawkmoth is able to generalize the olfactory stimulus of the plant through a spatiotemporal neural activation pattern elicited by a particular odorant blend or single compound in the first processing center of the insect brain, the antennal lobe (AL) (30–32). Activation patterns of the AL convey a message to higher olfactory centers of the brain eliciting a behavioral output. However, information from other sensory modalities may be integrated with olfactory information through multimodal mushroom body output neurons in these higher-order brain centers (33, 34). Experimental setups in the wind tunnel often set a minimized visual target and olfactory stimulus to measure feeding or oviposition behaviors; however, in an ecological context insect behaviors may be more adaptive through the use of multisensory stimuli (35–37).

The main olfactory structures are the antennae and maxillary (in Diptera) or labial (in Lepidoptera) palps on the insect head. There, odorants are mostly detected by chemosensory receptors belonging to membrane protein families of ionotropic receptors (IRs) and odorant receptors (ORs) (38, 39). IRs and ORs recognize specific volatile chemicals, resulting in the activation of associated olfactory sensory neurons (OSNs), which send axonal projections to the AL. Another large family of chemosensory membrane proteins, the gustatory receptors (GRs), are largely involved in contact (i.e., taste) chemoreception and are housed within gustatory organs such as the leg tarsi and the proboscis labella. In Lepidoptera, GRs play important roles in feeding and oviposition behaviors (40). Besides the detection of nonvolatile chemicals, GRs found in insect antennae or palps detect CO<sub>2</sub> (36, 41), which is a constituent of the *D. wrightii* floral volatile blend (42). IRs respond to volatile acids, amines, and aldehydes but are also involved in other sensory modalities, like thermo- and hygroreception (43–45). The 7 transmembrane ORs are involved in the majority of odorant detection. They colocalize with the conserved OR coreceptor (Orco), which serves as an obligatory chaperone for the localization and maintenance of ORs in the OSN membrane cilia (46, 47). On its own, Orco is a homotetramer that functions as a cation channel (48–52) with a pacemaker channel function controlling spontaneous activity of the OSN (53, 54). The precise role of the Orco–OR receptor complex in odorant signal transduction remains under debate (51, 55, 56). However, there is consensus in that the Orco–OR receptor complex binds a cognate ligand, resulting in the depolarization of the OSN. While ORs are highly diverse, for example there are 73 transcriptionally active ORs in both male and female *M. sexta* (57), there is only 1 evolutionarily highly conserved Orco (58–60).

The Orco gene null mutations among different insect orders are associated with a critical olfactory loss of function toward a broad range of odorants (47, 61–66). Additionally, olfactory-related behaviors such as short-distance orientation (47), host-chemical cue detection (61), pheromone detection (62, 64), and social communication (65, 66) are disrupted. We examined the role of OR-mediated olfaction within the *M. sexta*–*D. wrightii* interaction. We developed a specialized microinjection protocol for delivery of CRISPR–Cas9 ribonucleoprotein (RNP) complex to *M. sexta* embryos and generated an Orco knockout (KO) hawkmoth. The established *MsexOrco* null mutant, which was confirmed through genotyping and immunolocalization, lost pheromone detection and the male Orco KOs did not copulate, as observed in another moth species (62). The Orco KO individuals exhibited a deficiency in response to a selected panel of

odorants representative of *D. wrightii*-associated volatiles. We used the established Orco KO line to test the contribution of OR-dependent olfaction in foraging and oviposition behaviors using the natural multisensory stimulus of a whole potted *D. wrightii* plant. Our study offers an analysis of how ablation of OR-dependent olfaction affects foraging and oviposition behaviors of herbivorous insects.

## Results

**CRISPR–Cas9 Generation of *MsexOrco* Null Mutation.** We applied CRISPR–Cas9 to mutate *MsexOrco* and to obtain a nonfunctional Orco protein. The *M. sexta* Orco protein has 7 transmembrane regions and a molecular weight of ~54 kDa (54) (Fig. 1A). A 10-exon gene (*Msex2.12779*) in the official gene set 2 (OGS2) is predicted to encode *MsexOrco* (Fig. 1B, Top). It is located on the reverse strand of the JH668978.1 genomic scaffold. We used the CHOPCHOP v2 web tool on the OGS2 sequence data (67, 68) to identify CRISPR single-guide RNA (sgRNA) sequences against the second exon of the *MsexOrco*, based on reduced likelihood of off-target sites in the *M. sexta* genome. From multiple sgRNA candidates, we selected 2 that were situated on opposite strands of the second exon, 51 nucleotides apart from the respective CRISPR–Cas9 PAM sites (Fig. 1B). An RNP consisting of multiplexed sgRNAs in

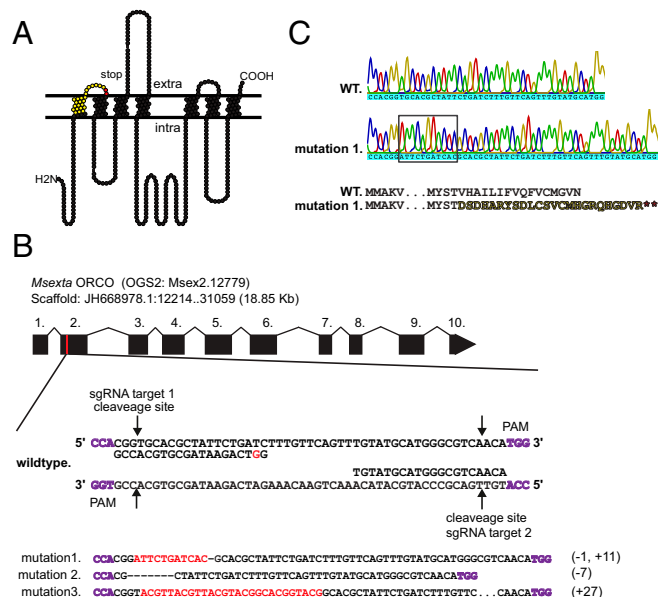


**Fig. 1.** CRISPR–Cas9-directed mutagenesis of *M. sexta* Orco. (A) The *M. sexta* Orco protein has 7 transmembrane domains. The first transmembrane domain was mutated generating a predicted frameshift (yellow) and translational stop signals (red) (B, Top). The *M. sexta* 10-exon Orco gene (18.85 kb) was accessed through the annotated official gene set (OGS) (gene ID *Msex2.12779*), with scaffold and base pair coordinate location on the positive strand (12,214 to 31,059 bp) within scaffold JH668978.1. A proximal region to the start of exon 2 was targeted for CRISPR single-guide RNA (sgRNA) design. Two sgRNAs (target1 and target2) on opposite DNA strands were multiplexed and injected. Target 1 was designed with a mismatch nucleotide, indicated in red to raise in vitro transcription efficiency. PAM sites indicated in purple, Cas9 cleavage sites 3 nucleotides from the PAM site indicated by arrows. (B, Bottom) Three germ-line insertion deletion (indel) mutations were recovered and sequenced (mutations 1, 2, and 3). All indels were generated by sgRNA target 1, insertion indicated in red, deletions indicated as dash lines. (C, Top) Mutation 1 was used for downstream functional analysis. Sanger sequencing chromatogram of wild-type (WT) individual and mutation 1 allele shows insertion event, indicated by box. (C, Bottom) Indel generated a frameshift mutation introducing 2 stop codons downstream, giving rise to a truncated 72-residue protein, indicated through the predicted amino acid sequence.

complex with the Cas9 enzyme was injected into 1- to 2-h-old eggs. We excised the second- to third-instar caterpillar horn tissue from surviving caterpillars ( $n = 42$ ) of 126 RNP-injected individuals. Using the T7 Endonuclease 1 (T7E1) assay on PCR product we were able to discern insertion-deletion (indel) mutations based on cleavage of heteroduplexed double-stranded DNA (SI Appendix, Fig. S1B). Of all injected parental generation ( $G^0$ ) caterpillars ( $n = 42$ ), 95% contained *MsexOrco* mutations.  $G^0$  individuals were back-crossed with wild-type (WT) hawkmoths, allowing the isolation and sequencing of germ-line mutations (SI Appendix, Fig. S1A). Inherited mutations were identified using T7E1 on the PCR product of first-generation ( $G^1$ ) colonies (SI Appendix, Fig. S1B). Three mutations from 3 separate parental pairs were identified by T7E1 digest of PCR product, cloning (TOPO-TA), and sequencing of positive individuals (Fig. 1 B, Bottom and SI Appendix, Fig. S1B). Mutation 1 was chosen based on both likelihood of functional consequences and feasible PCR-based genotyping (Fig. 1C). For this study, we chose an 11-bp insertion combined with a 1-bp deletion (Fig. 1 B and C, Top). The 11-bp with 1-bp deletion generated a frameshift with two premature stop signals on the predicted first extracellular loop (Fig. 1 A and C, Bottom).

**Neural Responses to Pheromones Are Abolished in Orco KO Hawkmoths.** A BclI restriction enzyme cutting site not found in the WT allele was introduced in the mutation 1, facilitating the identification of the KO allele. Individuals with the Orco KO allele produced a 160- and 52-bp PCR product (Fig. 2 A, Top); Orco KO was distinguishable from WT and Orco HET genotypes (Fig. 2 A, Bottom). The genotyped Orco KO was confirmed using immunohistochemistry. A polyclonal Orco primary antibody (54, 59) directed against the first intracellular loop of the Orco receptor protein in OSNs was used on WT male antennae (Fig. 2 B, Left). In contrast to WT antennae, no Orco-antibody labeling was identified in the Orco KO genotyped male antennae (Fig. 2 B, Right). To test for functional consequences of the *MsexOrco* mutation, we analyzed antennal and brain responses to the sex pheromone of genotyped individuals. The long trichoid sensilla of the *M. sexta* male antennae house 2 OSNs, 1 of which responds to the main female pheromone component bombykal (69, 70), detected by the pheromone receptor *MsexOR-1* (71). Single sensillum recordings from pheromone-sensitive trichoid sensilla in WT and Orco HET revealed significant responses to stimulation with 10E, 12Z-hexadecadienal (bombykal), while Orco KO showed no significant response (Fig. 2 C, Bottom). We tested the excised antennal response using electroantennograms (EAG). Male WT and Orco HET antennae exhibited significant responses of  $\sim 2$  mV to bombykal stimulations (Fig. 2 D, Top), while Orco KO responses to the pheromone were ablated (Fig. 2 D, Bottom). Next, we used  $Ca^{2+}$  imaging to investigate the AL responses of Orco KO hawkmoths. The AL receives projections from the antennal OSNs and is the first olfactory processing center of the insect brain. We visualized calcium-dependent activation patterns in the AL of WT ( $n = 4$ ) and Orco HET males ( $n = 4$ ) in response to stimulation with bombykal. In WTs, we found strong neural activity at the entrance region of the antennal nerve, where the pheromone processing macroglomerular complex (MGC) is located (72). In contrast, no such neural activity could be observed in the AL of Orco KO males ( $n = 4$ ) (SI Appendix, Fig. S3A). Also, morphological analysis of male ALs showed that the MGC, which is innervated by pheromone-sensitive OSNs (73), had a smaller relative volume in Orco KOs in comparison with WTs (SI Appendix, Fig. S3B). OR-mediated pheromone detection was absent in the Orco KO male hawkmoths. Thus, after genotyping each experimental animal, EAG recordings were employed in all adults stimulating with pheromones and other odorants, to further confirm the accuracy in all genotyped caterpillars ( $n_{\text{male}} = 88$ ;  $n_{\text{female}} = 191$ ).

**Orco KO Hawkmoths Showed Disrupted Responses toward *D. wrightii* Volatiles.** We investigated neuronal responses to host-plant odors to determine whether *M. sexta* Orco KO hawkmoths still detect *D. wrightii* odors. We analyzed AL responses to stimulation with headspace collected from flowering plants (SI Appendix, Fig. S4). We found extensive calcium responses associated with neuronal activity throughout the AL of both male and female WT and Orco HET hawkmoths, but no activity in the AL of Orco KO hawkmoths (Fig. 3A). Next, we tested the hawkmoth antennae with *D. wrightii* headspace and common floral and leaf volatile compounds as well as amines and acids to cover the typical response spectra of IRs (45, 74). The antennal responses to headspace and plant-related compounds in both male and female Orco KO hawkmoths were strongly reduced or absent (Fig. 3B and SI Appendix, Figs. S4 and S5 and Tables S2 and S3). However, responses to characteristic IR-mediated odors like benzaldehyde, hexanoic acid, and other acids and amines were still present, although reduced compared with the WT or Orco HET antenna. We next analyzed the activation pattern in the Orco KO AL for benzaldehyde, a floral volatile of *Datura*, and hexanoic acid, a compound emitted from the host plant (13) and associated with *M. sexta* herbivory (75). We found that although most of the activity elicited in WT and Orco HET hawkmoths had been lost, populations of neurons in a limited region opposite to the entrance of the antennal nerve were still activated (Fig. 3C). Glomeruli in this region were described to mainly respond to amines, acids, and aldehydes (31).

**Disrupted Odor-Directed Flight and Foraging Behaviors in the Orco KO Hawkmoths.** The mutualistic relationship between *M. sexta* and *D. wrightii* has been a focus of study in natural and laboratory settings, leading to various insights into the behavioral and sensory mechanisms involved in this interaction (3, 6, 11, 76, 77). After characterizing the Orco KO to *D. wrightii* headspace and representative odorants, we tested how these deficits affected the hawkmoth foraging behavior. We placed a *D. wrightii* plant with a single flower in a wind tunnel and released naive hawkmoths  $\sim 220$  cm downwind. Regardless of genotype nearly all tested male hawkmoths approached the flowering plant (Fig. 4A); for similar experiments with virgin females see SI Appendix, Fig. S7. However, Orco KO hawkmoths were slower from takeoff to first contact with the flower compared with both control genotypes (Fig. 4B and SI Appendix, Fig. S7B). The longer length of time it took the Orco KO hawkmoth to contact the flower was observed to be an effect of a prolonged searching behavior (Fig. 4C). The increased search time was not due to reduced motor function estimated by overall flight speed (SI Appendix, Fig. S8). The cumulative flight tracks showed that the Orco KO hawkmoths had a largely distributed residence time throughout the wind tunnel (Fig. 4D). Olfactory-directed flights have characteristic surge and casting behaviors when approaching an olfactory plume source upwind (25, 30). Analysis of the frequency of turn and counterturn angles of the flight tracks relative to the wind direction provides an image of a directed surge response toward the stimulus source ( $0^\circ$ ) (Fig. 4E). The WT and Orco HET male hawkmoths showed narrowing peak flight angles in line with the stimulus source. In the Orco KO these peaks appear distributed, indicating no characteristic odor-directed flight (Fig. 4E). When approaching the *D. wrightii* flower almost all WT and Orco HET hawkmoths unfurled their proboscis and probed the outer petals and the inner corolla (Fig. 4 F and G and SI Appendix, Fig. S7C and Movie S1). Furthermore, hawkmoths with extended proboscis often crawled in and out of the flower feeding on different nectar chambers within the *D. wrightii* flower. In contrast, the majority of Orco KO hawkmoths did not extend their proboscis but abruptly alighted on the flower or plant foliage (Fig. 4G and SI Appendix, Fig. S7C and Movie S1). Only 4 out of 31 tested male and female Orco KO individuals probed the flower with

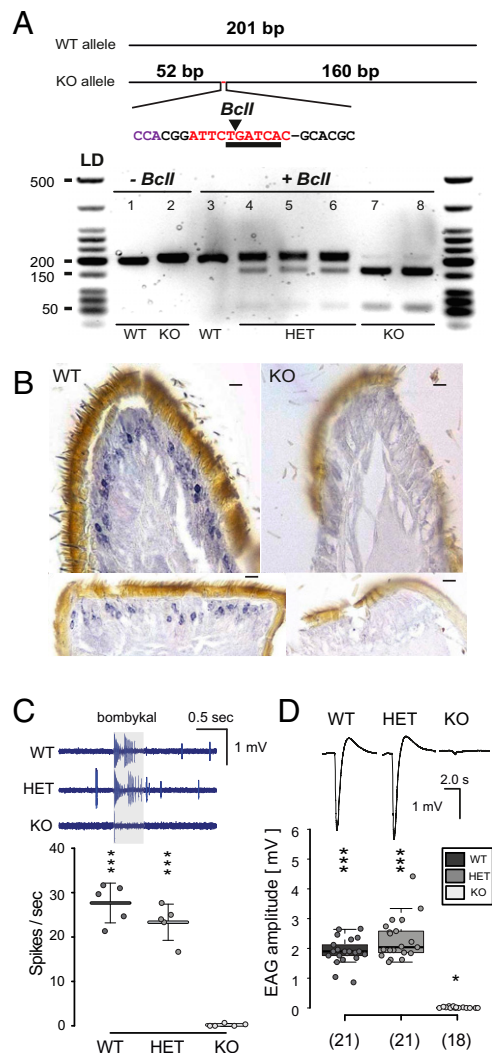


**Fig. 2.** Genotyped *M. sexta* Orco KOs do not express Orco or respond to conspecific female sex pheromone. (A, Top) Genotyping primers designed to amplify 201 bp of the targeted exon 2 of *MsexOrco*. Orco KO allele produces a 212-bp amplicon, characterized by the (–1, +11) indel, which introduces a *Bcl*I restriction enzyme cutting site not found in the WT allele. Insertion indicated in red, restriction site underlined, arrow points to enzymatic cut site. (A, Bottom) PCR product amplified from individual caterpillar horn tissue samples loaded on a 2.0% agarose gel. Lanes 1 and 2, PCR product with no restriction enzyme added. Lanes 3 through 8, PCR product cut with restriction enzyme. Lane 3, no cut bands from a WT caterpillar. Lanes 4 through 6, ~200-bp band of PCR product is still dark, with lighter bottom bands at ~150 and 50 bp, indicative of Orco HET individuals. Lanes 7 and 8, ~200 bp is mostly digested and breaks down to a darker ~150-bp band and ~50-bp band, indicative of the homozygous Orco KO individual. (B) Expression of the *M. sexta* Orco protein in the olfactory sensory neurons (OSNs) was characterized in the WT (Left) and KO (Right) on paraffin-embedded male antennae sections. Nickel-DAB staining with HRP conjugated secondary antibody detected Orco-positive OSNs only in the WT but not in Orco KO hawkmoths. Top, transversal; Bottom, sagittal sections. (Scale bars, 10  $\mu$ m.) (C) Single sensillum recordings (SSR) from long trichoid sensilla of adult male antennae stimulated with  $10^{-2}$  (vol/vol) bombykal in mineral oil for 0.5 ms. (Top) Representative SSR traces, odor stimulation indicated by the gray bar. (Bottom) Mean net responses from 3 sensilla per hawkmoth ( $\pm$  SD); circles represent results from individual hawkmoths. Total number of hawkmoths tested  $n = 5$  per genotype ( $***P \leq 0.001$ ; not significant,  $P \geq 0.05$ , 1-sample  $t$  test versus zero). (D) EAGs from clipped male antennae stimulated with bombykal; same concentration as in C. (Top) Representative EAG recordings. (Bottom) Box plots show the net response, corrected against solvent ( $*P \leq 0.05$ ,  $***P \leq 0.001$ , Wilcoxon rank sum test versus zero). Box plots show the median net EAG amplitude (horizontal line in the box), the 25th and 75th

their proboscis, 3 of which attempted to feed. This behavioral disruption likely indicates that although the *M. sexta* Orco KO hawkmoths were able to search and find the flower, they were unable to identify it as a nectar source.

### Oviposition Host-Seeking Behaviors Are Reduced; However, Orco KO Mated Hawkmoths Exhibited Characteristic Odor-Directed Flight.

Plant foliage volatile blends whether from intact (14) or larva-damaged plants (19–21) are an important factor in determining oviposition choice behaviors from the female *M. sexta*. To investigate if Orco is involved in mediating oviposition behaviors we thus exposed naïve mated female hawkmoths to a non-flowering *D. wrightii* plant in a wind tunnel. The Orco KO gravid females were less likely to make contact with the plant (Fig. 5A). However, the Orco KO females that approached the plant were as fast as the WT or Orco HET hawkmoths (Fig. 4B). The Orco KO gravid females displayed directed flight patterns to the plant similar to those of Orco HET and WT (Fig. 5C). They exhibited a cumulative flight distribution in the wind tunnel comparable to that of WT and Orco HET hawkmoths (Fig. 5D). The similar overall flight time and distribution was further substantiated by flight track angles in the Orco KO females, which showed odor-directed surged flight behavior toward the nonflowering plant similar to those of WT and Orco HET hawkmoths (Fig. 5E). Nearly all individuals that made contact with the plant oviposited; however, overall oviposition was affected by the significantly reduced number of hawkmoths that found the plant (Fig. 5F, white bar [KO], compared with Fig. 5A, white bar). Ovipositing females laid a similar number of eggs compared with the WT and Orco HET hawkmoths (Fig. 5G and Movie S2), indicating contact cues as crucial sensory stimuli for the oviposition response.

### Discussion

Understanding the role of olfaction in hawkmoth behavior requires the consideration of the multisensory ecological interaction with the host (77). We addressed these behaviors by generating an Orco KO hawkmoth with CRISPR-Cas9, therefore abolishing physiological and neuronal OR-mediated olfactory responses toward *D. wrightii* headspace and representative floral and vegetative volatiles. The Orco KO phenotype allowed us to quantify physiological responses toward certain acids and aldehydes. In the absence of Orco, foraging hawkmoths were still able to locate the flower, although their flight patterns and feeding behaviors were disrupted. Oviposition host-seeking behaviors were reduced as well; a significant number of hawkmoths could not locate the nonflowering plant. However, Orco KO hawkmoths that approached the plant demonstrated characteristic odor-directed flight behavior and oviposition. OR-dependent olfactory responses were clearly necessary for eliciting natural flower seeking and proboscis extension behaviors, while OR-independent olfactory responses appear to be additionally involved in female vegetative plant-seeking behaviors.

*D. wrightii* produces a flower with consistent visual, morphological, and olfactory characteristics, all used as sensory cues guiding hawkmoth pollination (8, 11). In general, animal-pollinated flowers tend to be conspicuous in terms of color, shape, texture, and odor gestalt (78, 79). The flower delivers a reliable multi-component signal ensuring pollination success; in turn, the insect relies on these signals to maximize nectar acquisition and to support metabolically costly searching behaviors (80–83). Our results, along with previous investigations (7, 84, 85), indicate that innate

percentiles (lower and upper margins of the box) together with the 1.5 $\times$  interquartile range (whiskers), and individual data points (circles). Genotyped individuals were all confirmed with EAG recordings, matching genotype to a physiological phenotype.

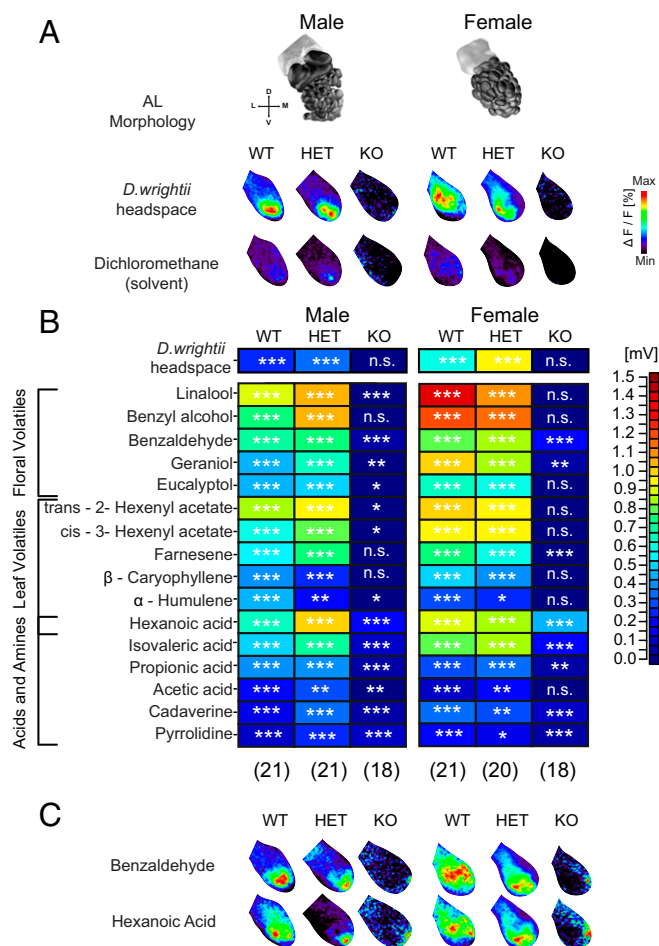


**Fig. 3.** *M. sexta* Orco KO show disrupted or reduced olfactory responses to plant headspace and to ecologically relevant single odors. (A) *D. wrightii* headspace collection was used to stimulate male and female antennae (for gas chromatogram see *SI Appendix*, Fig. S4). (Top) Presumed neural activity patterns from  $Ca^{2+}$  response in male and female antennal lobes (ALs) after stimulation with *D. wrightii* headspace in solvent. Pattern of responses varies based on sexual dimorphic morphology of the *M. sexta* AL (Top; ref. 119). False color-coded images are representative  $Ca^{2+}$  activity responses from right ALs; entrance of the antennal nerve is in the upper left. Images were generated by subtracting the frame before stimulus onset from the frame with the maximum response. Calcium activity was normalized for each image and color-coded (see color bar). (B) Heat-map representation of median EAG response values (millivolts) corrected for the response to the solvent from male and female antennae (\*\*\* $P \leq 0.001$ , \*\* $P \leq 0.01$ , \* $P \leq 0.05$ ; n.s., not significantly different from 0; Wilcoxon rank sum test versus zero). Box-plot representation and corrected median values with individual  $P$  values are shown in *SI Appendix*, Figs. S5 and S6 and Tables S2 and S3. Sample size of all 3 genotypes for headspace and single odorants male and female in parentheses ( $n$ ). (C) Neural activity in the AL of males and females in response to stimulation with benzaldehyde (floral odor) and hexanoic acid (vegetative odor) as these elicit the strongest EAG responses in the Orco KO hawkmoth.

behaviors involved in foraging–pollination-based mutualistic interactions are likely dependent on the stability between the visual stimulus and the appropriate floral volatile blend. Therefore, the coordination of different senses would have a direct advantage in generating an efficient behavioral output (35, 86). However, floral volatile blends are not always stable and can change based on herbivory or nectar availability (18, 87–89). Furthermore, the *D. wrightii* floral volatile blend is released at a much higher rate than the plant leaf volatiles (11). The females likely use these floral volatile signals as long-distance cues toward the plant and, additionally, foraging behaviors are observed to precede ovipo-

sition (11, 22). This interaction reveals further complexity in this insect–plant relationship where floral volatiles are not only used as foraging but also as oviposition cues. It was demonstrated that certain volatile compounds when altered in the *D. wrightii* floral blend had an effect on oviposition choice behaviors in female *M. sexta* (12, 22). Considering the critical nature of OR-related olfaction in foraging behaviors (Fig. 4 A and G), the disrupted sensory image of an altered volatile blend in combination with the visual input of the flower might also have a strong impact in determining preference behavior in a female hawkmoth.

The integration of multiple sensory inputs, including vision, is thought to effectively drive *M. sexta* foraging behaviors (84, 90). Observations in wind tunnels (with 2- to 3-m distance to the stimulus on release) or free-air fields (10 to 24 m) with natural or seminatural stimuli revealed that presenting the visual stimulus alone would result in *M. sexta* approaching the source but did not result in feeding (9, 85). In certain cases, only when an odor accompanied the visual stimulus was an approach followed by foraging attempts (91), determining that both cues are necessary for a hawkmoth to initiate and sustain foraging behavior (9, 84, 91). However, other studies using only an artificial visual stimulus, in a wind tunnel and a 1.5-m-diameter circular mesh arena, showed that the hawkmoth was able to extend its proboscis without a pronounced olfactory stimulus (8, 31, 92). In our study, we observe that disrupting the OR-mediated olfactory responses toward the flower significantly ablated proboscis extension and further foraging behaviors. The Orco KO hawkmoth exhibited an unusual behavior in the presence of natural innate stimuli: When approaching the flowering plant, they did not hover but instead landed abruptly. This behavior has not been previously reported, and we interpret this to be an effect of confronting the hawkmoth with a natural stimulus source with a disrupted olfactory identity. This also suggests that other present floral stimuli, such as relative humidity (93) and  $CO_2$  (76), were not sufficient to elicit feeding in the majority of hawkmoths. It is likely that the reluctance to forage at that moment is related to the sensory and neurobiological decoupling of vision and olfaction. Alternatively, while the flowering plant headspace did not elicit any responses from the antenna or AL, single odorants representative of the floral blend elicited minor responses from the Orco KO antenna at high concentrations. In the *M. sexta* AL, distinct regions remained activated in the Orco KO when certain odorants were used as stimuli (Fig. 3C), indicating putative glomeruli involved in IR-mediated responses. Therefore, the hawkmoth might have a residual detection of the flower likely determined through remaining IR-expressing olfactory neurons. However, this spatial pattern of activation is not representative of those eliciting proboscis extension behaviors (31, 32, 94). Additionally, odorants eliciting IR responses have been demonstrated to alter the valence property of that odorant in an Orco KO sensory background (45). The residual smell of the flower might simply be repulsive to the Orco KO hawkmoths.

Insects and plants have opposite interest regarding oviposition: The insect attempts to efficiently determine the most suitable host for its offspring, while the plant aims to prevent this approach. Changes in plant volatile blends can have drastic effects on oviposition choice behaviors, providing a defensive strategy for the plant. Multiple genetic and environmental factors qualitatively and quantitatively influence the *D. wrightii* constitutive plant foliage volatile blend (95–97), delivering variable olfactory signals. In general, leaf volatile profiles change due to the time of day (98), plant genotype (99), interplant communications (100), and other biotic and abiotic stress-induced conditions (101–103). Orco is likely involved in the detection of many of these volatiles (Fig. 3B) (27); however, we demonstrate that some female hawkmoths were able to use odor-directed flight independent of Orco (Fig. 5E), suggesting an additional sensory input in this insect–plant interaction. These OR-independent signals could be used by the hawkmoth as

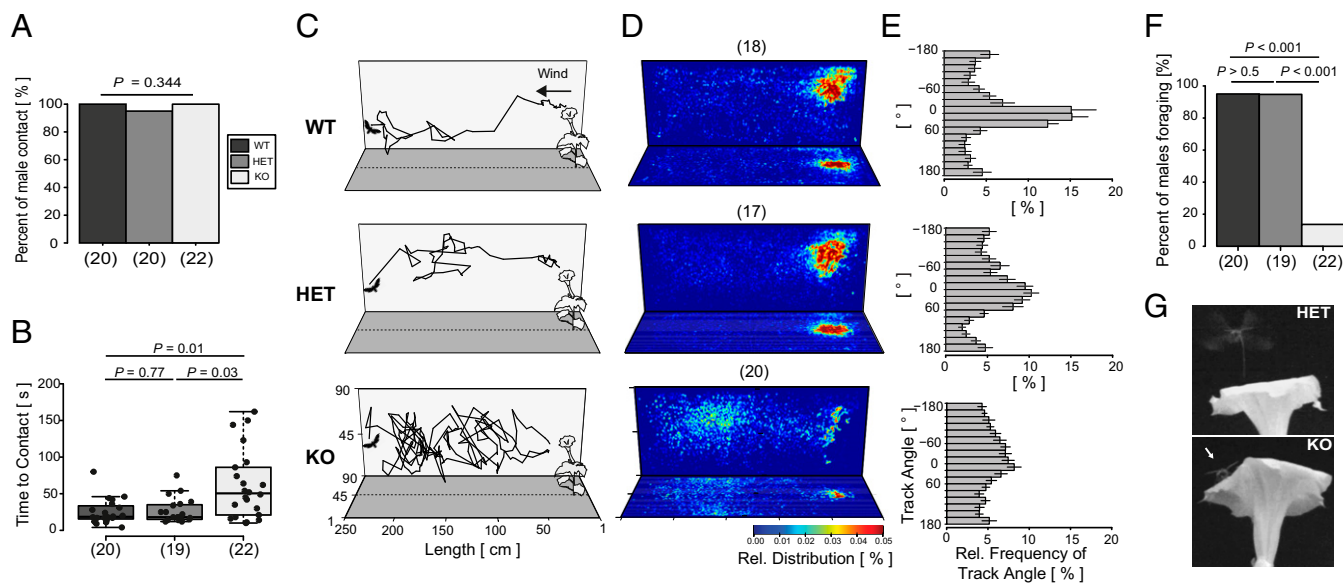


**Fig. 4.** *M. sexta* Orco KO were slower to reach a flowering plant and showed disrupted foraging. (A) The percentage of male hawkmoths that flew toward a flowering *D. wrightii* plant (stimulus source) in a 250-cm-long wind tunnel did not differ between genotypes. Total number of hawkmoths tested ( $n$ ) in parentheses. ( $\chi^2 = 2.1344$ ; degrees of freedom = 2; test of equal proportions). (B) Orco KO hawkmoths took longer to contact the plant. The time to contact was calculated from take-off until males hovered in front of the flower or contacted the plant in a 5-min free-flight experiment (Holm corrected Wilcoxon rank sum test). The box plots show the median net contact time (horizontal line in the box), the 25th and 75th percentiles (lower and upper margins of the box) together with the 1.5 $\times$  interquartile range (whiskers), and individual data points (circles). (C) Three-dimensional flight tracks in response to the stimulus source, hawkmoth (not to scale) depicts start of flight toward nonflowering plant (not to scale) in a wind tunnel. Flight tracks were chosen based on time to contact median values. (D) Two-dimensional heat map representation of the cumulative relative distribution of all tracked hawkmoths from start to stimulus source; sample size ( $n$ ). Single pixels represent points of relative transit of the hawkmoth color-coded from maximum transit (red) to no transit (dark blue) (see color bar). (E) The relative frequency of track-angle (flight direction relative to the wind) toward the flowering plant is shown as the percentages of track angles toward stimulus source ( $0^\circ$ ). (F) Percentage of free-flight males that foraged was significantly reduced in the Orco KO males compared with WT and Orco HET. Foraging counted when males unfurled the proboscis and contacted the flower with the proboscis ( $\chi^2 = 41.118$ ; degrees of freedom = 2;  $P < 0.001$ ; Holm corrected test of equal proportions). (G) Images captured from an infrared filter camera above the flower in wind tunnel flight experiments. Orco HET male with proboscis extended preparing to forage (Top) and Orco KO male immediately after contacting the flower, without proboscis extended (Bottom).

an alternative sensory stimulus when seeking out a host plant. This suggests a flexible sensory response in oviposition behaviors that could be used to overcome the variability of plant volatile blends.

Female hawkmoths are adapted to process olfactory information from plant odor plumes as a guide toward specific host plants. Sexually dimorphic small trichoid sensilla found on the female antennae house OSNs broadly tuned to a subset of plant volatiles: terpenoids and aromatics (27). In our experiment, 61% of gravid females were able to quickly locate a *D. wrightii* non-flowering plant in a characteristic olfactory-directed flight pattern independent of OR-mediated olfaction (Fig. 5 B and E), indicating that other sensory mechanisms might play important roles in this flight behavior. One possibility would be IR-mediated olfaction. IRs are an ancient chemosensory receptor gene family in arthropods (104) and IR-mediated olfaction is independent of Orco. IRs expressed in the antennae of the vinegar fly, *Drosophila melanogaster*, are involved in the detection of humidity and temperature, in addition to subsets of chemical volatiles (43, 45, 105). Our results indicate significant antennal responses from Orco KO female hawkmoths to certain putative IR-detected class of odorants (Fig. 3B and SI Appendix, Fig. S6 and Table S3). However, antenna and AL responses toward *D. wrightii* plant-related volatiles such as hexanoic acid and benzaldehyde (13, 75, 106) are reduced, indicating Orco-dependent detection contributing to the full physiological response. Many IR genes are conserved between the vinegar fly and the hawkmoth (57), but the role of IRs in the detection of plant leaf compounds has not yet been explored. Benzaldehyde is a compound of the *Datura* floral blend; however, it is also found in the vegetative plant volatile profile (13). Six carbon aldehydes are part of the “green leaf” odor blend both humans and insects

detect from plants (17, 107). IRs in the antennae of the vinegar fly detect these plant leaf aldehydes (45). Additionally, locust mouthparts appear to use Orco-independent olfaction for the detection of these compounds (108). The hawkmoth might also be employing an IR-dependent mechanism of hygrosensation (43) to identify the relative humidity from plant leaf transpiration in their host-seeking behaviors. Vision is also a relevant ecological and short-distance behavioral stimulus for *M. sexta* (109). Hawkmoths are able to employ color reception in directing their behaviors (110–112) and recent studies have observed how ambient light affects *M. sexta* color discrimination and host localization (113, 114). However, it is not clear if *M. sexta* can use any of these visual sensory stimuli in the detection of color or contrast image of a nonflowering plant.

The relationship between *M. sexta* and *D. wrightii* is one of plant chemical signals and insect chemosensory detection. Analyzing the precise contribution of each sense is informative on how insects and plants use and manipulate signals to enhance their overall fitness. With the *M. sexta* Orco KO we observed a contextual dependency on OR-based olfaction in this relationship. In foraging, the critical nature of olfaction is likely governed through the integration of visual and olfactory stimuli to elicit the complete range of foraging behavior. The coupling between vision and olfaction in this behavior highlights the evolutionary link between floral shape and color with scent for *M. sexta* pollinated flowers (7, 84). On the other hand, the decoupling of OR-mediated olfaction from oviposition behaviors might favor innate adaptability toward other potential signals. Without Orco the female hawkmoth is able to use other sensory signals exclusively to locate the plant, demonstrating a flexible multisensory mechanism for female host-seeking behaviors. Our

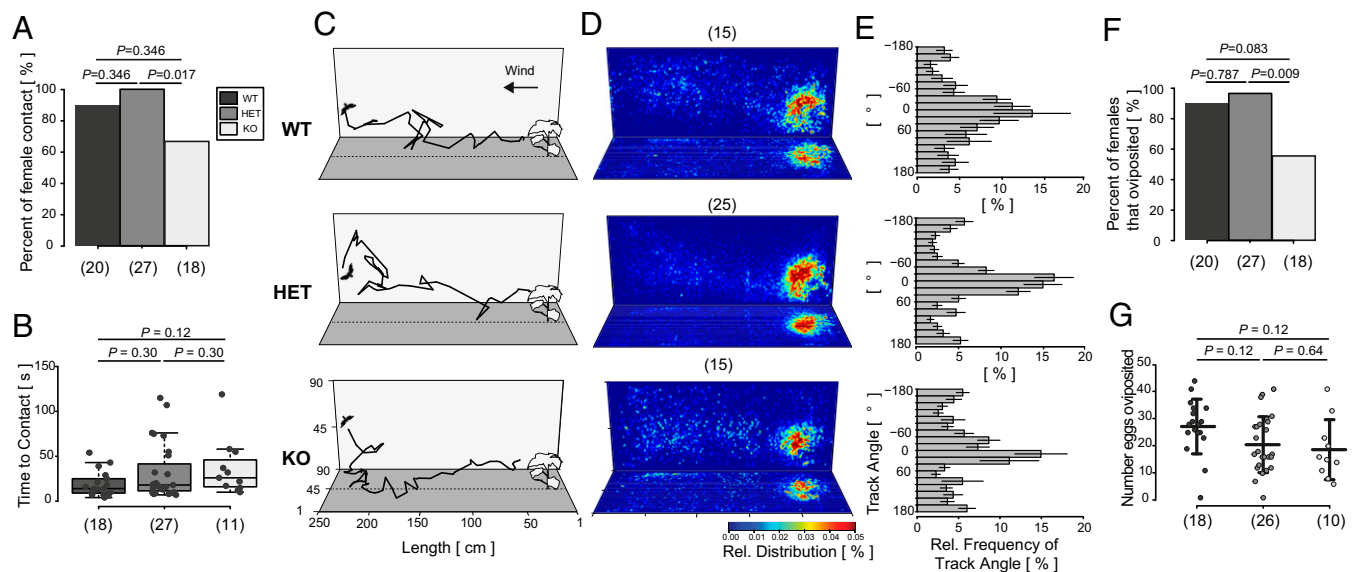


**Fig. 5.** Orco KO gravid hawkmoths have reduced attraction toward nonflowering *D. wrightii*; however, females that flew to the plant used olfactory-directed flight behaviors. (A) The percentage of mated *M. sexta* females that flew and contacted a nonflowering *D. wrightii* plant (stimulus source) was significantly reduced in KOs compared with WT and HET females ( $\chi^2 = 11.261$ ; degrees of freedom = 2;  $P = 0.004$ ; Holm corrected test of equal proportions). (B) Time to contact was measured from take-off to physical contact on the plant. Orco KO female time to the stimulus source was not significantly different compared with WT and Orco HET (Kruskal–Wallis H test). Box plots show the median net contact time (horizontal line in the box), the 25th and 75th percentiles (lower and upper margins of the box) together with the 1.5 $\times$  interquartile range (whiskers), and individual data points (circles). (C) Three-dimensional flight tracks in response to the plant stimulus, hawkmoth (not to scale) depicts start of flight toward nonflowering plant (not to scale). Flight tracks were chosen based on time to contact median values. (D) Two-dimensional heat map representation of the cumulative relative distribution of all tracked hawkmoths data from start to source; sample size ( $n$ ). Single pixels represent points of relative transit of the hawkmoth color-coded from maximum transit (red) to no transit (dark blue) (see color bar). (E) The relative frequency of track angle (flight direction relative to the wind) toward the nonflowering plant is shown as the percentages of track angles toward stimulus source (0°). (F) The percentage of total females that elicited oviposition behaviors (contact on leaf and abdomen curl) on whole *D. wrightii* plant were significantly reduced in the KOs compared with HET or WT females ( $\chi^2 = 13.735$ ; degrees of freedom = 2;  $P = 0.001$ ; Holm corrected test of equal proportions). (G) Fifty-five percent of total Orco KO females laid a similar number of eggs on *D. wrightii* plants compared with WT and Orco HET. Bars and error bars represent mean  $\pm$  SD, with no significant differences between genotypes (not significant; one-way ANOVA).

study presents another step in understanding the link between neurobiology and ecology through the application of CRISPR-Cas9 to classic ecological models. It allows us to speculate on a role for olfaction in the life history of a hawkmoth and how it might have adapted through the course of coevolution. The development of feasible germ-line cell transformation will permit future studies in applying transgenic tools to further explore the neurobiology of coevolved behaviors shaping our natural heritage and agriculture.

## Materials and Methods

Procedures for *M. sexta* CRISPR-Cas9 sgRNA design and functional verification, *M. sexta* and *D. wrightii* general colony rearing, volatile collection and analysis, AL calcium imaging odorant stimulation, image analysis, and wind-tunnel staging and 3D tracking are described in *SI Appendix, Supplementary Methods*.

***M. sexta* Preblastoderm Microinjection, Embryo Staging, and Rearing.** Eggs for microinjection were collected from a breeding chamber with a potted *D. wrightii* plant placed 15 min before the simulated dusk conditions. Eggs were processed for microinjection 1 to 2 h postoviposition. Freshly laid eggs were collected after 15-min bouts of oviposition and stored at 5 °C until sufficient eggs were accumulated. Eggs were washed thoroughly with distilled water in a *Drosophila* egg lay cup with a mesh screen (Genesee Scientific; [Flystuff.com](http://Flystuff.com)), followed by 5-min incubation in 2% Comma's brilliant blue stain (50% methanol vol/vol and 10% glacial acetic acid vol/vol). The Comma's blue treatment facilitates evaluation of *M. sexta* egg polarity based on the staining and visualization of the micropyle under a stereomicroscope (Leica S8APO; Leica), in addition to softening the egg shell for injection (115). The eggs were washed thoroughly in distilled water and dried on tissue paper before staging. Eggs were aligned on a microscope slide dressed with double-sided tape and lined up against a longwise strip of Erkogum or clay. Eggs were placed with posterior side relative the micropyle (anterior) facing out based on the probability of this region developing the

germ plasm determinants (116). While some Lepidoptera species like *Bombyx mori* have been shown to have an alternate method of embryonic pre patterning, *M. sexta* has been demonstrated to follow a similar pathway to that of *Drosophila* (117, 118).

**Embryo Microinjection.** Eggs were injected with a short taper quartz glass capillary with filament (inside diameter 1.0 mm and outside diameter 1.0 mm; Sutter Instruments) pulled with a Sutter P-2000 laser puller (1 line: heat = 700; filament = 2; velocity = 30; delay = 130; pull = 75) (Sutter Instruments). The underside of the glass slide with eggs was adhered with water to the glass stage plate on a Zeiss AxioZoom V16 stereomicroscope fitted with an aureka digital micromanipulator (Aura Optik) set at a 45° angle. A Narishige IM-300 microinjector (Narishige) with nitrogen-sourced pressure standing at 62.0 psi and an initial pressure of 20.0 psi was used during initial injection with further adjustments, as needed, down to 2.0 psi. The pressure was lowered to adjust to the fine capillary tip breaking off from repeated injection but maintains a thin enough taper to keep injecting with high survivability. After injection, wounds were sealed with cyanoacrylate adhesive (Loctite 401; Henkel) and the slide was placed in a fly vial with a wet cotton bottom and a sponge stopper; eggs were then placed in a climate chamber.

**Rearing of Injected Colony.** On day 3 postinjection eggs were gently removed from the slide and placed on a Petri dish in proximity to a small amount of larval artificial diet. Freshly hatched larvae were separated into small cups (Solo 1.25-ounce soufflé cups) with diet and sealed with custom-cut cardboard lids. Larvae were transferred to a small 250-mL plastic salad boxes after reaching third instar and fed for ad libitum consumption, refreshing food when needed. Wandering stage larvae were separated into a new plastic tub with tissue paper and transferred to brown paper bags 2 wk later.

**Genetic Crosses.** One male and 1 female hawkmoth were placed in a mesh screen cage (30  $\times$  30  $\times$  30 cm) to mate (*SI Appendix, Fig. S1 and Table S1*). A *D. wrightii* leaf or paper towel was placed 1 to 2 d later to collect eggs. Eggs were placed in a plastic cup with label of parental generation and the current

progeny colony name. Once larvae hatched from the eggs, individuals were separated in to small plastic cups for genotyping.

***M. sexta* Genotyping and Phenotyping.** A 1.0-mm section of caterpillar horn from second- to third-instar larvae was harvested and placed in a 96-well plate with 10.0  $\mu$ L of MyTaq Extract-PCR Kit Lysis buffer (2  $\mu$ L buffer A, 1  $\mu$ L buffer B, and 7  $\mu$ L double-distilled H<sub>2</sub>O, modified protocol from Bioline; Meridian Life Sciences). Tissue was homogenized using a wet toothpick to quickly press the horn tissue to the side of the well or by cutting the horn multiple times in the lysis buffer. A nested PCR (*SI Appendix, Table S4*) using MyTaq HS Red Mix (Bioline) was necessary for a sufficient amplification of a 920-bp region flanking the gRNA1 target site. The nested PCR provided an approximate equivalent amplification needed for T7E1 (NEB). The resulting digest was visualized on a 1.5% agarose gel. PCR-amplified DNA from T7E1 digest positive individuals of the G1 generation was cloned into Dual Promoter TA Cloning Kit pCRII Vector (Invitrogen; ThermoFisher Scientific). Multiple colonies were picked for each cloning reaction, amplified, and purified in a 96-well plate and sequenced at the Max Planck Institute for Chemical Ecology. Sequenced data were analyzed using Geneious version 8 (Biomatters). Three sequences, hence three colonies, with positive indel mutations were confirmed by sequencing (*SI Appendix, Fig. S1*); once these individuals were back-crossed to WT male *M. sexta* the rest were disposed of by freezing. Minimal colonies were maintained because of space limitations in the climate chamber. Position of this frameshift mutation was identified using TOPCONS2 to predict the *M. sexta* Orco topology and illustrated using Protter (<http://wlab.ethz.ch/protter>) (Fig. 1A). Once the G<sup>2</sup> generation of

colony 1 was confirmed by T7E1 the other colonies were discarded. The stochastic insertion of a BclI site in colony 1 facilitates the identification of HET and KO individuals from the WT individuals. To maintain the following generations for experimental purposes primers were designed to amplify 201 bp (*SI Appendix, Table S4*) with the target site or mutation located 50 bp downstream from the 5' of the PCR amplicon. A 10- $\mu$ L BclI digest (5  $\mu$ L PCR template, 1  $\mu$ L NEB3.1 buffer, 0.25 BclI, and 3.75 double-distilled H<sub>2</sub>O) reaction was set up from the PCR and loaded on a 2% agarose gel. Every subsequent generation requires identification of HET and KO individuals using BclI digest. Accuracy of genotyping method was examined by EAG characterization of individual hawkmoths after behavioral experimentation. Either the full panel of odorants (Fig. 2B) or a selection of 5 diagnostic odors (bombykal, hexanoic acid, linalool, pyrrolidine, and benzyl alcohol) was used to match antennal responses to genotyped individuals.

**ACKNOWLEDGMENTS.** This work was funded by the Max Planck Society and in part by the Deutsche Forschungsgemeinschaft STE531/20-1,2 (to M.S., K.S., and A.W.). We thank Dr. U. Müller, Dr. R. Kipper, and Aura Optik for developing micromanipulation for the AxioZoom v16 (Zeiss); Dr. N. Gompel and Dr. A. Martin for helpful suggestions with microinjection and CRISPR-Cas9; Dr. T. G. Montague for uploading the *M. sexta* OGS2 for the CHOP-CHOP web-tool; Dr. J. Weißflog and Dr. A. Svatos for synthesizing pheromone; Dr. J. Krieger for providing antibody; Dr. G. Kunert for advice with statistics; Dr. D. Kessler and the Max Planck Institute for Chemical Ecology greenhouse staff for supplying *D. wrightii* plants; Katharina Heise and Till Kalkreuter for AL reconstructions and measurements; and Sylke Diemel and Angela Lehman for assistance with *M. sexta* rearing and genotyping.

1. J. Visser, Host odor perception in phytophagous insects. *Annu. Rev. Entomol.* **31**, 121–144 (1986).
2. B. S. Hansson, M. C. Stensmyr, Evolution of insect olfaction. *Neuron* **72**, 698–711 (2011).
3. J. L. Bronstein, T. Huxman, B. Horvath, M. Farabee, G. Davidowitz, Reproductive biology of *Datura wrightii*: The benefits of a herbivorous pollinator. *Ann. Bot.* **103**, 1435–1443 (2009).
4. J. L. Bronstein, The costs of mutualism. *Am. Zool.* **41**, 825–839 (2001).
5. V. Grant, Behavior of hawkmoths on flowers of *Datura meteloides*. *Bot. Gaz.* **144**, 280–284 (1983).
6. J. A. Riffell *et al.*, Behavioral consequences of innate preferences and olfactory learning in hawkmoth-flower interactions. *Proc. Natl. Acad. Sci. U.S.A.* **105**, 3404–3409 (2008).
7. R. A. Raguso, M. A. Willis, Synergy between visual and olfactory cues in nectar feeding by wild hawkmoths, *Manduca sexta*. *Anim. Behav.* **69**, 407–418 (2005).
8. J. A. Riffell, R. Alarcón, Multimodal floral signals and moth foraging decisions. *PLoS One* **8**, e72809 (2013).
9. A. Haverkamp *et al.*, Hawkmoths evaluate scenting flowers with the tip of their proboscis. *eLife* **5**, 1–12 (2016).
10. J. Goyret, R. A. Raguso, The role of mechanosensory input in flower handling efficiency and learning by *Manduca sexta*. *J. Exp. Biol.* **209**, 1585–1593 (2006).
11. R. A. Raguso, C. Henzel, S. L. Buchmann, G. P. Nabhan, Trumpet flowers of the sonoran desert: Floral biology of *Peniocereus cacti* and sacred *Datura*. *Int. J. Plant Sci.* **164**, 877–892 (2003).
12. C. E. Reisenman, J. A. Riffell, E. A. Bernays, J. G. Hildebrand, Antagonistic effects of floral scent in an insect-plant interaction. *Proc. Biol. Sci.* **277**, 2371–2379 (2010).
13. A. Späthe *et al.*, Plant species- and status-specific odorant blends guide oviposition choice in the moth *Manduca sexta*. *Chem. Senses* **38**, 147–159 (2013).
14. W. L. Mechaber, C. T. Capaldo, J. G. Hildebrand, Behavioral responses of adult female tobacco hornworms, *Manduca sexta*, to hostplant volatiles change with age and mating status. *J. Insect Sci.* **2**, 5 (2002).
15. A. M. Fraser, W. L. Mechaber, J. G. Hildebrand, Electroantennographic and behavioral responses of the sphinx moth *Manduca sexta* to host plant headspace volatiles. *J. Chem. Ecol.* **29**, 1813–1833 (2003).
16. R. T. Yamamoto, R. Y. Jenkins, R. K. McClusky, Factors determining the selection of plants for oviposition by the tobacco hornworm. *Entomol. Exp. Appl.* **12**, 504–508 (1969).
17. S. Allmann, I. T. Baldwin, Insects betray themselves in nature to predators by rapid isomerization of green leaf volatiles. *Science* **329**, 1075–1078 (2010).
18. M. Dicke, I. T. Baldwin, The evolutionary context for herbivore-induced plant volatiles: Beyond the 'cry for help'. *Trends Plant Sci.* **15**, 167–175 (2010).
19. A. Kessler, I. T. Baldwin, Defensive function of herbivore-induced plant volatile emissions in nature. *Science* **291**, 2141–2144 (2001).
20. S. Allmann *et al.*, Feeding-induced rearrangement of green leaf volatiles reduces moth oviposition. *eLife* **2**, e00421 (2013). Erratum in: *eLife* **2**, e00992 (2013).
21. C. M. De Moraes, M. C. Mescher, J. H. Tumlinson, Caterpillar-induced nocturnal plant volatiles repel conspecific females. *Nature* **410**, 577–580 (2001).
22. C. E. Reisenman, J. A. Riffell, J. G. Hildebrand, Neuroethology of oviposition behavior in the moth *Manduca sexta*. *Ann. N. Y. Acad. Sci.* **1170**, 462–467 (2009).
23. N. J. Vickers, T. C. Baker, Iterative responses to single strands of odor promote sustained upwind flight and odor source location by moths. *Proc. Natl. Acad. Sci. U.S.A.* **91**, 5756–5760 (1994).
24. I. Beyaert, M. Hilker, Plant odour plumes as mediators of plant-insect interactions. *Biol. Rev. Camb. Philos. Soc.* **89**, 68–81 (2014).
25. R. T. Cardé, M. A. Willis, Navigational strategies used by insects to find distant, wind-borne sources of odor. *J. Chem. Ecol.* **34**, 854–866 (2008).
26. M. Ghaninia, S. B. Olsson, B. S. Hansson, Physiological organization and topographic mapping of the antennal olfactory sensory neurons in female hawkmoths, *Manduca sexta*. *Chem. Senses* **39**, 655–671 (2014).
27. V. D. C. Shields, J. G. Hildebrand, Responses of a population of antennal olfactory receptor cells in the female moth *Manduca sexta* to plant-associated volatile organic compounds. *J. Comp. Physiol. A Neuroethol. Sens. Neural Behav. Physiol.* **186**, 1135–1151 (2001).
28. B. S. Hansson, M. A. Carlsson, B. Kalinowski, Olfactory activation patterns in the antennal lobe of the sphinx moth, *Manduca sexta*. *J. Comp. Physiol. A Neuroethol. Sens. Neural Behav. Physiol.* **189**, 301–308 (2003).
29. J. A. Riffell *et al.*, Sensory biology. Flower discrimination by pollinators in a dynamic chemical environment. *Science* **344**, 1515–1518 (2014).
30. J. A. Riffell, H. Lei, J. G. Hildebrand, Neural correlates of behavior in the moth *Manduca sexta* in response to complex odors. *Proc. Natl. Acad. Sci. U.S.A.* **106**, 19219–19226 (2009).
31. S. Bisch-Knaden, A. Dahake, S. Sachse, M. Knaden, B. S. Hansson, Spatial representation of feeding and oviposition odors in the brain of a hawkmoth. *Cell Rep.* **22**, 2482–2492 (2018).
32. J. A. Riffell, H. Lei, T. A. Christensen, J. G. Hildebrand, Characterization and coding of behaviorally significant odor mixtures. *Curr. Biol.* **19**, 335–340 (2009).
33. M. F. Strube-Bloss, W. Rössler, Multimodal integration and stimulus categorization in putative mushroom body output neurons of the honeybee. *R. Soc. Open Sci.* **5**, 171785 (2018).
34. A. Balkenius, S. Bisch-Knaden, B. Hansson, Interaction of visual and odour cues in the mushroom body of the hawkmoth *Manduca sexta*. *J. Exp. Biol.* **212**, 535–541 (2009).
35. E. A. Hebets, D. R. Papaj, Complex signal function: Developing a framework of testable hypotheses. *Behav. Ecol. Sociobiol.* **57**, 197–214 (2005).
36. C. J. McMeniman, R. A. Corfas, B. J. Matthews, S. A. Ritchie, L. B. Vosshall, Multimodal integration of carbon dioxide and other sensory cues drives mosquito attraction to humans. *Cell* **156**, 1060–1071 (2014).
37. S. B. Ramaswamy, Host finding by moths: Sensory modalities and behaviours. *J. Insect Physiol.* **34**, 235–249 (1988).
38. L. B. Vosshall, R. F. Stocker, Molecular architecture of smell and taste in *Drosophila*. *Annu. Rev. Neurosci.* **30**, 505–533 (2007).
39. R. Benton, K. S. Vannice, C. Gomez-Diaz, L. B. Vosshall, Variant ionotropic glutamate receptors as chemosensory receptors in *Drosophila*. *Cell* **136**, 149–162 (2009).
40. A. R. Agnihotri, A. A. Roy, R. S. Joshi, Gustatory receptors in Lepidoptera: Chemosensation and beyond. *Insect Mol. Biol.* **25**, 519–529 (2016).
41. W. D. Jones, P. Cayirlioglu, I. G. Kadow, L. B. Vosshall, Two chemosensory receptors together mediate carbon dioxide detection in *Drosophila*. *Nature* **445**, 86–90 (2007).
42. P. G. Guerenstein, E. A. Yezep, J. Van Haren, D. G. Williams, J. G. Hildebrand, Floral CO<sub>2</sub> emission may indicate food abundance to nectar-feeding moths. *Naturwissenschaften* **91**, 329–333 (2004).
43. Z. A. Knecht *et al.*, Ionotropic Receptor-dependent moist and dry cells control hygrosensation in *Drosophila*. *eLife* **6**, 1–11 (2017).
44. R. Rytz, V. Croset, R. Benton, Ionotropic receptors (IRs): Chemosensory ionotropic glutamate receptors in *Drosophila* and beyond. *Insect Biochem. Mol. Biol.* **43**, 888–897 (2013).
45. A. F. Silbering *et al.*, Complementary function and integrated wiring of the evolutionarily distinct *Drosophila* olfactory subsystems. *J. Neurosci.* **31**, 13357–13375 (2011).
46. R. Benton, S. Sachse, S. W. Michnick, L. B. Vosshall, Atypical membrane topology and heteromeric function of *Drosophila* odorant receptors in vivo. *PLoS Biol.* **4**, e20 (2006).
47. M. C. Larsson *et al.*, Or83b encodes a broadly expressed odorant receptor essential for *Drosophila* olfaction. *Neuron* **43**, 703–714 (2004).



48. J. A. Butterwick *et al.*, Cryo-EM structure of the insect olfactory receptor Orco. *Nature* **560**, 447–452 (2018).
49. L. Mukunda, S. Lavista-Llanos, B. S. Hansson, D. Wicher, Dimerisation of the *Drosophila* odorant coreceptor Orco. *Front. Cell. Neurosci.* **8**, 261 (2014).
50. D. Wicher *et al.*, *Drosophila* odorant receptors are both ligand-gated and cyclic-nucleotide-activated cation channels. *Nature* **452**, 1007–1011 (2008).
51. K. Sato *et al.*, Insect olfactory receptors are heteromeric ligand-gated ion channels. *Nature* **452**, 1002–1006 (2008).
52. M. Stengl, N. W. Funk, The role of the coreceptor Orco in insect olfactory transduction. *J. Comp. Physiol. A Neuroethol. Sens. Neural Behav. Physiol.* **199**, 897–909 (2013).
53. A. Nolte *et al.*, In situ tip-recordings found no evidence for an Orco-based ionotropic mechanism of pheromone-transduction in *Manduca sexta*. *PLoS One* **8**, e62648 (2013).
54. A. Nolte *et al.*, No evidence for ionotropic pheromone transduction in the hawkmoth *Manduca sexta*. *PLoS One* **11**, e0166060 (2016).
55. R. Smart *et al.*, *Drosophila* odorant receptors are novel seven transmembrane domain proteins that can signal independently of heterotrimeric G proteins. *Insect Biochem. Mol. Biol.* **38**, 770–780 (2008).
56. P. L. Jones, G. M. Pask, D. C. Rinker, L. J. Zwiebel, Functional agonism of insect odorant receptor ion channels. *Proc. Natl. Acad. Sci. U.S.A.* **108**, 8821–8825 (2011).
57. C. Koenig *et al.*, A reference gene set for chemosensory receptor genes of *Manduca sexta*. *Insect Biochem. Mol. Biol.* **66**, 51–63 (2015).
58. W. D. Jones, T. A. T. Nguyen, B. Kloss, K. J. Lee, L. B. Vosshall, Functional conservation of an insect odorant receptor gene across 250 million years of evolution. *Curr. Biol.* **15**, R119–R121 (2005).
59. J. Krieger, O. Klink, K. Mohl, K. Raming, H. Breer, A candidate olfactory receptor subtype highly conserved across different insect orders. *J. Comp. Physiol. A Neuroethol. Sens. Neural Behav. Physiol.* **189**, 519–526 (2003).
60. C. Missbach *et al.*, Evolution of insect olfactory receptors. *eLife* **3**, e02115 (2014). Erratum in: *eLife* **3**, e05087 (2014).
61. M. DeGennaro *et al.*, Orco mutant mosquitoes lose strong preference for humans and are not repelled by volatile DEET. *Nature* **498**, 487–491 (2013).
62. F. A. Koutroumpa *et al.*, Heritable genome editing with CRISPR/Cas9 induces anosmia in a crop pest moth. *Sci. Rep.* **6**, 29620 (2016).
63. Y. Li *et al.*, CRISPR/Cas9 in locusts: Successful establishment of an olfactory deficiency line by targeting the mutagenesis of an odorant receptor co-receptor (Orco). *Insect Biochem. Mol. Biol.* **79**, 27–35 (2016).
64. Q. Liu *et al.*, Deletion of the *Bombyx mori* odorant receptor co-receptor (BmOrco) impairs olfactory sensitivity in silkworms. *Insect Biochem. Mol. Biol.* **86**, 58–67 (2017).
65. W. Tribble *et al.*, Orco mutagenesis causes loss of antennal lobe glomeruli and impaired social behavior in ants. *Cell* **170**, 727–735.e10 (2017).
66. H. Yan *et al.*, An engineered orco mutation produces aberrant social behavior and defective neural development in ants. *Cell* **170**, 736–747.e9 (2017).
67. K. Labun, T. G. Montague, J. A. Gagnon, S. B. Thyme, E. Valen, CHOPCHOP v2: A web tool for the next generation of CRISPR genome engineering. *Nucleic Acids Res.* **44**, W272–W276 (2016).
68. T. G. Montague, J. M. Cruz, J. A. Gagnon, G. M. Church, E. Valen, CHOPCHOP: A CRISPR/Cas9 and TALEN web tool for genome editing. *Nucleic Acids Res.* **42**, W401–W407 (2014).
69. K. Kaissling, J. G. Hildebrand, J. H. Tumlinson, Pheromone receptor cells in the male moth *Manduca sexta*. *Arch. Insect Biochem. Physiol.* **10**, 273–279 (1989).
70. B. Kalinová, M. Hoskovec, I. Liblikas, C. R. Unelius, B. S. Hansson, Detection of sex pheromone components in *Manduca sexta* (L.). *Chem. Senses* **26**, 1175–1186 (2001).
71. D. Wicher *et al.*, Identification and characterization of the bombykal receptor in the hawkmoth *Manduca sexta*. *J. Exp. Biol.* **220**, 1781–1786 (2017).
72. S. Matsumoto, J. Hildebrand, Olfactory interneurons in the moth *Manduca sexta*: Response characteristics and morphology of central neurons in the antennal lobes. *Proc. R. Soc. London Ser. B Biol. Sci.* **213**, 249–277 (1981).
73. B. S. Hansson, T. A. Christensen, J. G. Hildebrand, Functionally distinct subdivisions of the macroglomerular complex in the antennal lobe of the male sphinx moth *Manduca sexta*. *J. Comp. Neurol.* **312**, 264–278 (1991).
74. J. Knudsen, L. Tollsten, Trends in floral scent chemistry in pollination syndromes: Floral scent composition in moth-pollinated taxa. *Bot. J. Linn. Soc.* **113**, 263–284 (1993).
75. A. Weinhold, I. T. Baldwin, Trichome-derived O-acyl sugars are a first meal for caterpillars that tags them for predation. *Proc. Natl. Acad. Sci. U.S.A.* **108**, 7855–7859 (2011).
76. C. Thom, P. G. Guerenstein, W. L. Mechaber, J. G. Hildebrand, Floral CO<sub>2</sub> reveals flower profitability to moths. *J. Chem. Ecol.* **30**, 1285–1288 (2004).
77. A. L. Stöckl, A. Kelber, Fuelling on the wing: Sensory ecology of hawkmoth foraging. *J. Comp. Physiol. A Neuroethol. Sens. Neural Behav. Physiol.* **205**, 399–413 (2019).
78. A. S. Leonard, A. Dornhaus, D. R. Papaj, “Why are floral signals complex? An outline of functional hypotheses” in *Evolution of Plant-Pollinator Relationships*, S. Patiny, Ed. (Cambridge University Press, Cambridge, 2011), pp. 279–300.
79. R. A. Raguso, R. A. Levin, S. E. Foose, M. W. Holmberg, L. A. McDade, Fragrance chemistry, nocturnal rhythms and pollination “syndromes” in *Nicotiana*. *Phytochemistry* **63**, 265–284 (2003).
80. H. G. Baker, Evolutionary mechanisms in pollination biology: Origins and functions of floral systems are being elucidated by genetical and ecological studies. *Science* **139**, 877–883 (1963).
81. T. M. Casey, Flight energetics of sphinx moths: Power input during hovering flight. *J. Exp. Biol.* **64**, 529–543 (1976).
82. A. Haverkamp, J. Bing, E. Badeke, B. S. Hansson, M. Knaden, Innate olfactory preferences for flowers matching proboscis length ensure optimal energy gain in a hawkmoth. *Nat. Commun.* **7**, 11644 (2016).
83. A. S. Leonard, A. Dornhaus, D. R. Papaj, Flowers help bees cope with uncertainty: Signal detection and the function of floral complexity. *J. Exp. Biol.* **214**, 113–121 (2011).
84. R. A. Raguso, M. A. Willis, Synergy between visual and olfactory cues in nectar feeding by naïve hawkmoths, *Manduca sexta*. *Anim. Behav.* **64**, 685–695 (2002).
85. R. A. Raguso, M. A. Willis, “Hawkmoth pollination in Arizona’s Sonoran Desert: Behavioral responses to floral traits” in *Butterflies: Evolution and Ecology Taking Flight*, C. L. Boggs, W. B. Watt, P. R. Erlich, Eds. (University of Chicago Press, 2003), pp. 43–65.
86. G. Gingras, B. A. Rowland, B. E. Stein, The differing impact of multisensory and unisensory integration on behavior. *J. Neurosci.* **29**, 4897–4902 (2009).
87. L. A. Burkle, J. B. Runyon, Drought and leaf herbivory influence floral volatiles and pollinator attraction. *Glob. Change Biol.* **22**, 1644–1654 (2016).
88. D. Kessler, C. Diezel, D. G. Clark, T. A. Colquhoun, I. T. Baldwin, *Petunia* flowers solve the defence/apparency dilemma of pollinator attraction by deploying complex floral blends. *Ecol. Lett.* **16**, 299–306 (2013).
89. F. P. Schiestl, M. Ayasse, H. F. Paulus, D. Erdmann, W. Francke, Variation of floral scent emission and postpollination changes in individual flowers of *Ophrys sphegodes* subsp. *sphogodes*. *J. Chem. Ecol.* **23**, 2881–2895 (1997).
90. A. Balkenius, M. Dacke, Learning of multi-modal stimuli in hawkmoths. *PLoS One* **8**, e71137 (2013).
91. J. Goyret, P. M. Markwell, R. A. Raguso, The effect of decoupling olfactory and visual stimuli on the foraging behavior of *Manduca sexta*. *J. Exp. Biol.* **210**, 1398–1405 (2007).
92. A. Balkenius, M. Dacke, Flight behaviour of the hawkmoth *Manduca sexta* towards unimodal and multimodal targets. *J. Exp. Biol.* **213**, 3741–3747 (2010).
93. M. von Arx, J. Goyret, G. Davidowitz, R. A. Raguso, Floral humidity as a reliable sensory cue for profitability assessment by nectar-foraging hawkmoths. *Proc. Natl. Acad. Sci. U.S.A.* **109**, 9471–9476 (2012).
94. J. A. Riffell, H. Lei, L. Abrell, J. G. Hildebrand, Neural basis of a pollinator’s buffet: Olfactory specialization and learning in *Manduca sexta*. *Science* **339**, 200–204 (2013).
95. J. D. Hare, Variation in herbivore and methyl jasmonate-induced volatiles among genetic lines of *Datura wrightii*. *J. Chem. Ecol.* **33**, 2028–2043 (2007).
96. H. M. Kruidhof, J. D. Allison, J. D. Hare, Abiotic induction affects the costs and benefits of inducible herbivore defenses in *Datura wrightii*. *J. Chem. Ecol.* **38**, 1215–1224 (2012).
97. A. Olcerst, “Variation in induced responses of *Datura wrightii* to herbivore attack: Plasticity of volatile organic compound emissions and gene expression across genotypes, ontogeny, and a single attack,” PhD dissertation, University of California, Riverside (2017).
98. M. C. Schuman, H. A. Valim, Y. Joo, “Temporal dynamics of plant volatiles: Mechanistic bases and functional consequences” in *Deciphering Chemical Language of Plant Communication*, J. D. Blande, R. Glinwood, Eds. (Springer International Publishing, Cham, 2016), pp. 3–34.
99. R. Halitschke, A. Kefler, J. Kahl, A. Lorenz, I. T. Baldwin, Ecophysiological comparison of direct and indirect defenses in *Nicotiana attenuata*. *Oecologia* **124**, 408–417 (2000).
100. E. Pezzola, S. Mancuso, R. Karban, Precipitation affects plant communication and defense. *Ecology* **98**, 1693–1699 (2017).
101. Y. Aartsma, F. J. J. A. Bianchi, W. van der Werf, E. H. Poelman, M. Dicke, Herbivore-induced plant volatiles and tritrophic interactions across spatial scales. *New Phytol.* **216**, 1054–1063 (2017).
102. E. H. Poelman *et al.*, Field parasitism rates of caterpillars on Brassica oleracea plants are reliably predicted by differential attraction of *Cotesia* parasitoids. *Funct. Ecol.* **23**, 951–962 (2009).
103. B. Niederbacher, J. B. Winkler, J. P. Schnitzler, Volatile organic compounds as non-invasive markers for plant phenotyping. *J. Exp. Bot.* **66**, 5403–5416 (2015).
104. V. Crosset *et al.*, Ancient protostome origin of chemosensory ionotropic glutamate receptors and the evolution of insect taste and olfaction. *PLoS Genet.* **6**, e1001064 (2010).
105. G. Budelli *et al.*, Ionotropic receptors specify the morphogenesis of phasic sensors controlling rapid thermal preference in *Drosophila*. *Neuron* **101**, 738–747.e3 (2019).
106. B. Vicedo *et al.*, Hexanoic acid-induced resistance against *Botrytis cinerea* in tomato plants. *Mol. Plant Microbe Interact.* **22**, 1455–1465 (2009).
107. A. Hatanaka, The biogenesis of green odour by green leaves. *Phytochemistry* **34**, 1201–1218 (1993).
108. L. Zhang, H. Li, L. Zhang, Two olfactory pathways to detect aldehydes on locust mouthpart. *Int. J. Biol. Sci.* **13**, 759–771 (2017).
109. A. Balkenius, C. Balkenius, Behaviour towards an unpreferred colour: Can green flowers attract foraging hawkmoths? *J. Exp. Biol.* **213**, 3257–3262 (2010).
110. A. Balkenius, W. Rosén, A. Kelber, The relative importance of olfaction and vision in a diurnal and a nocturnal hawkmoth. *J. Comp. Physiol. A Neuroethol. Sens. Neural Behav. Physiol.* **192**, 431–437 (2006).
111. A. Kelber, Ovipositing butterflies use a red receptor to see green. *J. Exp. Biol.* **202**, 2619–2630 (1999).
112. A. Kelber, A. Balkenius, E. J. Warrant, Scotopic colour vision in nocturnal hawkmoths. *Nature* **419**, 922–925 (2002).
113. J. Goyret, M. L. Yuan, Influence of ambient illumination on the use of olfactory and visual signals by a nocturnal hawkmoth during close-range foraging. *Integr. Comp. Biol.* **55**, 486–494 (2015).
114. W. Kuenzinger *et al.*, Innate colour preferences of a hawkmoth depend on visual context. *Biol. Lett.* **15**, 20180886 (2019).
115. R. Yanagimachi *et al.*, Sperm attractant in the micropyle region of fish and insect eggs. *Biol. Reprod.* **88**, 47 (2013).
116. B. Ewen-Campen, E. E. Schwager, C. G. Extavour, The molecular machinery of germ line specification. *Mol. Reprod. Dev.* **77**, 3–18 (2010).
117. R. Kraft, H. Jäckle, *Drosophila* mode of metamerization in the embryogenesis of the lepidopteran insect *Manduca sexta*. *Proc. Natl. Acad. Sci. U.S.A.* **91**, 6634–6638 (1994).
118. H. Nakao, M. Hatakeyama, J. M. Lee, M. Shimoda, T. Kanda, Expression pattern of *Bombyx vasa*-like (BmVGL) protein and its implications in germ cell development. *Dev. Genes Evol.* **216**, 94–99 (2006).
119. Grosse-Wilde *et al.*, Antennal transcriptome of *Manduca sexta*. *Proc. Natl. Acad. Sci. U.S.A.* **108**, 7449–7454 (2011).